Lecture Notes in Networks and Systems 1035

Jawad Rasheed
Adnan M. Abu-Mahfouz
Muhammad Fahim *Editors*

Forthcoming Networks and Sustainability in the AIoT Era

Second International Conference FoNeS-AIoT 2024 – Volume 1

Springer

Lecture Notes in Networks and Systems 1035

The series "Lecture Notes in Networks and Systems" publishes the latest developments in Networks and Systems—quickly, informally and with high quality. Original research reported in proceedings and post-proceedings represents the core of LNNS.

Volumes published in LNNS embrace all aspects and subfields of, as well as new challenges in, Networks and Systems.

The series contains proceedings and edited volumes in systems and networks, spanning the areas of Cyber-Physical Systems, Autonomous Systems, Sensor Networks, Control Systems, Energy Systems, Automotive Systems, Biological Systems, Vehicular Networking and Connected Vehicles, Aerospace Systems, Automation, Manufacturing, Smart Grids, Nonlinear Systems, Power Systems, Robotics, Social Systems, Economic Systems and other. Of particular value to both the contributors and the readership are the short publication timeframe and the world-wide distribution and exposure which enable both a wide and rapid dissemination of research output.

The series covers the theory, applications, and perspectives on the state of the art and future developments relevant to systems and networks, decision making, control, complex processes and related areas, as embedded in the fields of interdisciplinary and applied sciences, engineering, computer science, physics, economics, social, and life sciences, as well as the paradigms and methodologies behind them.

Indexed by SCOPUS, INSPEC, WTI Frankfurt eG, zbMATH, SCImago.

All books published in the series are submitted for consideration in Web of Science.

For proposals from Asia please contact Aninda Bose (aninda.bose@springer.com).

Jawad Rasheed · Adnan M. Abu-Mahfouz ·
Muhammad Fahim
Editors

Forthcoming Networks and Sustainability in the AIoT Era

Second International Conference FoNeS-AIoT 2024 – Volume 1

Springer

Editors
Jawad Rasheed
Department of Computer Engineering
Istanbul Sabahattin Zaim University
Istanbul, Türkiye

Muhammad Fahim
School of Electronics, Electrical Engineering
and Computer Science
Queen's University Belfast
Belfast, UK

Adnan M. Abu-Mahfouz
Council for Scientific and Industrial Research
(CSIR)
Pretoria, South Africa

Department of Electrical and Electronic
Engineering Science
University of Johannesburg
Johannesburg, South Africa

ISSN 2367-3370 ISSN 2367-3389 (electronic)
Lecture Notes in Networks and Systems
ISBN 978-3-031-62870-2 ISBN 978-3-031-62871-9 (eBook)
https://doi.org/10.1007/978-3-031-62871-9

This Springer imprint is published by the registered company Springer Nature Switzerland AG
The registered company address is: Gewerbestrasse 11, 6330 Cham, Switzerland

Contents

Determining the Digits of Turkish Sign Languages Using Deep Learning Techniques

Emine Karataş and Gökalp Çınarer(✉)

Yozgat Bozok University, Yozgat, Turkey
gokalp.cinarer@bozok.edu.tr

Abstract. Sign language is a physical language that enables people with disabilities to communicate with each other by using hand and facial movements as a whole to express themselves. It is very important that sign language is learned by everyone and used as a communication tool for the disabled to adapt to social life and to express themselves easily. For this reason, people's learning of sign languages, which are specific to the country's spoken language, will increase the quality of life of people with disabilities. In this study, 12981 images of the numbers 0–10 in Turkish Sign Language taken from different angles were used as a data set. In the last stage of the study, the detection of digits over images was carried out with CNN, Resnet-50, VGG-16, Densenet-201, and Inception-V3 deep learning architectures. In the study, an effective model of deep learning algorithms is proposed to determine which number an action corresponds to in sign language. Examining the models, VGG-16 and Densenet-201 were the architectures that gave the highest accuracy with 100% accuracy. After these architectures, Inception-V3 architecture comes with 99.91% success in determining the numbers. It has been seen that it is very successful in detecting numbers in Turkish Sign Language using deep learning models.

Keywords: Hand Gesture Recognition · Sign Language Translation · Deep Learning

1 Introduction

Sign language vital tool that deaf people make use of to express themselves using body language [1]. It is necessary to know sign language correctly and evaluate its importance accordingly. Even though deaf people can communicate with each other through sign language, people who go to public or private places have difficulty explaining themselves and understanding others. As stated by the findings of the research carried out by the World Health Organization in Europe in 2018, 34 million people with hearing impairment have been identified. It is estimated that this number will approach 46 million in 2050 [2].

Hearing-impaired people were cut off from social life until recently. It has been mentioned in the studies that hearing-impaired individuals from different communities have difficulty communicating even among themselves, despite participating in international sports-related events together [3, 4]. In addition, in Gondon's research, he stated

J. Rasheed et al. (Eds.): FoNeS-AIoT 2024, LNNS 1035, pp. 1–10, 2024.
https://doi.org/10.1007/978-3-031-62871-9_1

that there are more than 124 sign languages in the world and that individuals from different nationalities have problems in communicating even if they have similar aspects [5]. The World Report on the Disabled states that individuals with hearing impairments generally have difficulty interpreting sign language. According to a study involving 93 countries, translation services are not available in 31 countries and the number of translators authorized for translation services in 30 countries is 20 or less. With the developing technology, it is necessary to benefit from artificial intelligence technologies to eliminate such problems.

In this study, the success of deep learning architectures in detecting numbers from 0 to 10 for Turkish Sign Language has been examined.

2 Literature Review

In the literature research, deep learning is exploited in several fields such as software industry [6], image processing [7], and noise detection [8], however, it is seen that the studies on sign language are quite limited in Turkey. On the other hand, the number of studies in this field in the USA is quite high. Ravinder Ahuja proposed a model for performing gesture recognition of American Sign Language using a Convolutional Neural Network (CNN). They evaluated 24 hand signals in the study where they used the user's camera recordings. At the end of the study, they reached an accuracy rate of 99,7% [9]. Abdulwahap et al. used CNN deep learning architecture to classify American letters and got a result of 99.33%. They revealed that they got a higher result for CNN when compared with SVM and ANN algorithms [10].

In another study, Indian Sign Language alphabets and numbers were used. To train 36 static movements, a classification process was performed using 45,000 RGB and 45,000 depth images with CNN architecture. As a result of the training, 98.81% accuracy was obtained. [11].

Selvi and Kemaloğlu [12] classified Turkish sign language digits with the CNN and reached a test accuracy of 98.55%. Fernandez and Kwolek presented a CNN-based algorithm for hand gesture recognition from a color camera. They used 6000 tagged images. They were labeled in 10 classes. They did their work on CNN and completed their work with a high degree of accuracy [13].

Rahmat and his team have signed two separate studies. In the first study, 6 different hand movements were carried out, for the second study, 4 different hand movements were performed. The most successful test result from the study was obtained from the test performed for four different hand movement types. In the study 300 and 50 hidden neurons were used for each layer, in two hidden layers [14].

In another study [15], 99.90% training accuracy was achieved in the classification made with 35,000 images of facial static signs. In a study conducted with the Arabic sign language recognition method, in a study that recognized 32 hand gestures, the VGG16 and ResNet152 models reached 99% accuracy [16].

A comparative analysis of similar studies in the literature is shown in Table 1. On the other side sample images of numbers used in Turkish sign language are given in Table 2.

Table 1. Studies examined in the literature.

Project Owners	Study Content	Method	Truth
Aeshita Mathur et al. [17]	Containing 500 images for 26 English Alphabets	CNN VGG16	91.16%
Yao-Liang Chung [18]	Contains 4800 images for numbers 1–5 hand gesture recognition system	CNN VVGNET	95.61%
Müneer El Hammadi and team [19]	A sign language definition study was conducted with 5 words taken from 40 participants	3D CNN	96.69%
Molchanov and team [20]	20,000 images of 10 static digits	CNN	97.62%
Islam and team [21]	1075 image Bangla Sign Language 10 static digits	CNN	95%

Table 2. Sample images of numbers used in Turkish sign language.

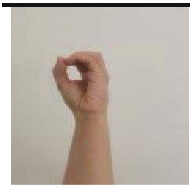 0	 1	 2
 3	 4	 5
 6	 7	 8
 9	 10	

3 Material and Method

3.1 Dataset

The data set consists of 12981 images of Turkish sign language containing numbers between 0 and 10. Images were obtained with a 1080p resolution camera, at a frame rate of 30fps, at a focal length of 26 mm, in a plain background font, in RGB color. Images are in 3000x4000 pixel size, jpeg file format. In the study, 12981 images of 11 classes, taken from a person, from a background, and at distances ranging from 0 to 30 cm from the camera, were obtained on a plain white background and in-room conditions. The dataset is divided into 10695 images for train and 2286 images for test.

3.2 Deep Learning

Deep learning is a data modeling system developed as a sub-branch of machine learning in which different neuron layers are used, influenced by the human brain. Multiple neuron layers are designed with different methods and analyzed with different parameters.

In systems developed according to the size of the dataset, the depth of the network is optimized accordingly, and high accuracy is tried to be achieved in complex classifications. According to the weights created during the training, the data is processed in the hidden layers, their features are extracted, and predictions are made. Unlike traditional machine learning methods, the whole system evaluates the features it automatically obtains instead of manually extracting the data. Thus, it can also be applied in multi-class and complex structures. The class and complex structures. The algorithm used in all these processes can be supervised or unsupervised depending on the state of the data. As the similarities of the pictures increase, the performance of CNN architectures decreases [22]. In addition, representation learning, and classification categories are automatically discovered in the machine's processing of raw data [23].

3.3 Convolutional Neural Network (CNN)

CNN is one of the basic architectures of Deep Learning. Inspired by the way animals see. Its use has become widespread in many fields. Although it is preferred in fields such as audio processing, natural language processing, and biomedical, it gives the highest accuracy in image processing. It simplifies complex operations using convolution filters. CNN image classifications take input data, process it, and categorize it under certain categories [24]. A standard CNN architecture is a set of feedforward layers that implement convolutional filters and pool layers. After the last pooling layer, CNN uses several fully connected layers to classify the map features of the previous layers. Does not require a feature extraction before CNN architecture is implemented [25].

In a feedforward neural network, any middle layer is called hidden because the activation function and the final convolution layer mask the input and output. The layers that enable the formation of convolutions contain hidden layers [26].

In summary, ESAs consist of several trainable parts in a row. Then, classification is done with an educational classifier. In ESA, the training process starts with receiving the input data and continues by processing layer by layer. This is how the training process ends. A block diagram of the Turkish Sign Language recognition system is given in Fig. 1.

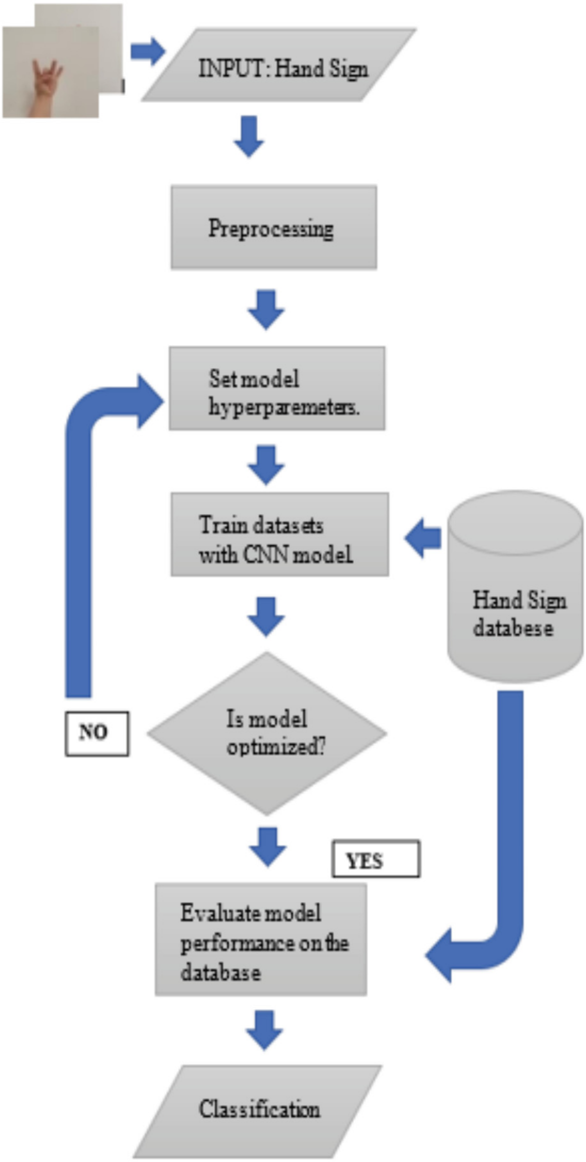

Fig. 1. Block diagram of Turkish Sign Language recognition system.

As the last operation, it gives the final output for comparison with the correct result. It is also very important how many pieces of data will be processed simultaneously in the training of the model. Here batch size values need to be defined in each architecture. Like the epoch number, the batch size is a hyperparameter with no rules. Conversely, if a batch size is too large, it may not fit in the memory of the computational sample used for training and will tend to overfit the data. It is important to note that batch size affects other hyper-parameters such as learning rate, so the combination of these hyper-parameters is just as important as the batch size itself. The main purpose of hyperparameters is to determine the variables of the best performance achieved [27].

To evaluate and validate the effectiveness of the proposed approaches, experiments were performed in 10 and 30 epochs, respectively. Parameters and hyperparameters were tried to raise the performance of the model, and the ones with the highest results were used in the project. Basic parameters like the number of layers, filters, and the optimization applied were taken into account in the performance analysis. Classification processes were performed on images using the Resnet-50, VGG16, Densenet-201, and InceptionV3 architectures.

4 Results and Discussion

For the detection of hand movements in sign language, a CNN model was created and the classification process was carried out for the numbers between "0–10". Google Colaboratory environment was used for training. Google Colaboratory is a system created for use in artificial intelligence studies. It is a Jupyter Notebook environment running in the cloud. By making the necessary distinction and classification in the data set Google Drive environment, for numbers between 0 and 10, "zero: 0, one: 1, two: 2, three: 3, four: 4, five: 5, six: 6, seven: 7, eight: 8, nine: 9, ten: 10" in the form of train and test. The dataset is divided into 80% for train and 20% for test.

In the study, architectures were run in two ways, 10 epochs and 30 epochs. An epoch ends when the dataset has been transmitted back and forth over the neural network exactly once. The success of the model is tested. Weights are updated accordingly. This process is repeated in each epoch. There is no rule for choosing the epoch number. This is a hyperparameter that must be determined before training begins. As the accuracy values increase, the decrease in the loss values shows that the architectures make a successful classification.

Train accuracy and validation accuracy results are shown in the same graph. As a result of the experiment, the success and loss-loss graphs of the test and training data at the end of 30 epochs of deep learning architectures are shown in Fig. 2.

Basic performance parameters were used to evaluate the validity and performance of this study.

The results of the algorithms running 10 epochs and 30 epochs for each evaluation metric and the architectures used are given in detail in Table 3. When the performances of the models were compared, it was seen that some models reached 100% accuracy and some architectures changed their accuracy according to the number of epochs. Looking at Table 3, it appears that the accuracy of VGG-16 and DenseNet-201 architectures increased after 30 epochs.

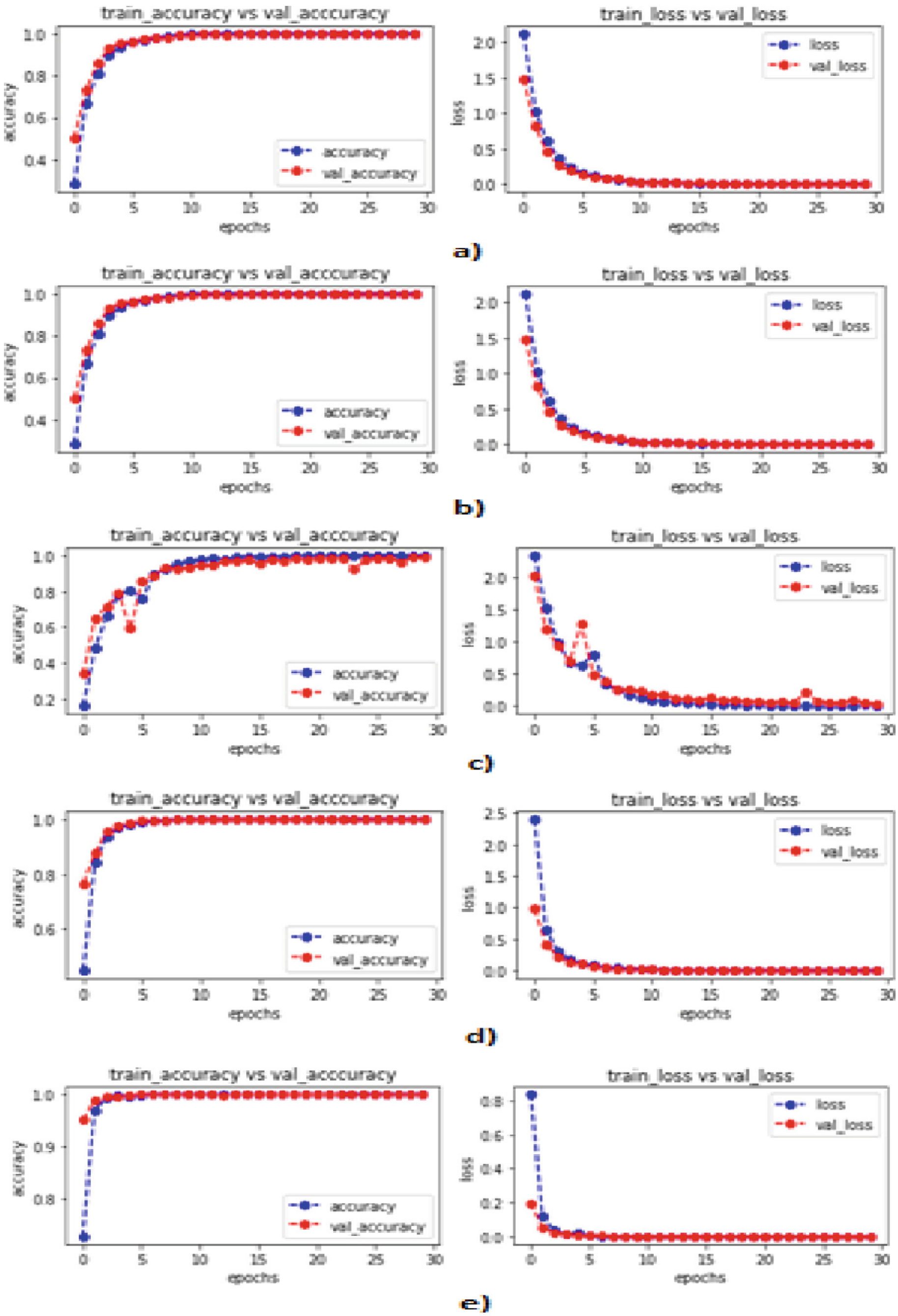

Fig. 2. Performance analysis graphs of models a) CNN b) VGG16 c) Resnet50 d) DenseNet201 e) InceptionV3

While there is a slight decrease in CNN and Resnet-50 architectures, it is seen that the accuracy value of the Inception-V3 architecture does not change. The fact that the number of classes is eleven is effective in the high classification success of the numbers. As the number of classes increases, the complexity will increase, so there will be changes in the accuracy values of the architectures.

Table 3. Accuracy rates of models.

Model	Accuracy (10 epoch)	Accuracy (30 epoch)
CNN	98,99	99,83
VGG-16	99,95	100
DENSENET-201	99,65	100
RESNET-50	98,95	98,86
INCEPTION-V3	99,91	99,91

Precision, recall, and F1-score values of the architectures are given in Table 4. It was observed that the architectures distinguished all 11 classes with high accuracy at the end of 30 epochs.

Table 4. Performance rates of models with 30 epochs.

Model	Precision	Recall	F1 Score
CNN	0,99	0,99	0,99
VGG-16	1,00	1,00	1,00
DENSENET-201	1,00	1,00	1,00
RESNET-50	0,99	0,99	0,99
INCEPTION-V3	1,00	1,00	1,00

5 Conclusion

In this study, recognition of Turkish Sign Language numbers with hand gestures is carried out with different deep learning architecture. It has been seen that the hand movements taken from different angles in the dataset created within the scope of the research are classified with high accuracy by the architectures. This study reveals that Turkish sign language numbers can be recognized by different convolutional neural networks. When the experimental results were examined, it was observed that the recognition performance of CNN architectures increased considering that the images were shot in a similar environment. Application of the proposed system with different hand movements and under different conditions may change the results.

It has been classified with higher accuracy than studies conducted in other different languages. The basic parameters that the architectures use while determining this affect the classification success. When the models were examined, VGG-16 and Densenet-201 were the architectures that gave the highest accuracy with 100% accuracy. Next comes the Inception-V3 architecture with 99.91%. In future studies, studies can be carried out with images including letters and numbers in different conditions. Turkish sign language numerals and the Turkish sign language alphabet can be compared with different datasets with new methods and models. In addition, different CNN architectures that can increase accurate prediction can be used in studies.

References

1. Sangeethalakshmi, K., Shanthi, K.G., Raj, A.M., Muthuselvan, S., Taha, P.M., Shoaib, S.M.: Hand gesture vocalizer for deaf and dumb people. Mater. Today Proc. **80**, 3589–3593 (2023)
2. Yildiz, Z., Yildiz, S., Bozyer, S.: İşitme Engelli Turizmi (Sessiz Turizm): Dünya ve Türkiye Potansiyeline Yönelik Bir Değerlendirme. Süleyman Demirel Üniversitesi Vizyoner Dergisi **9**(20), 103–117 (2018)
3. Theunissen, S.C., et al.: Self-esteem in hearing-impaired children: the influence of communication, education, and audiological characteristics. PLoS ONE **9**(4), e94521 (2014)
4. Morata, T.C., Themann, C.L., Randolph, R.F., Verbsky, B.L., Byrne, D.C., Reeves, E.R.: Working in noise with a hearing loss: perceptions from workers, supervisors, and hearing conservation program managers. Ear Hear. **26**(6), 529–545 (2005)
5. Gordon, R.G., Jr. ed.: Ethnologue: Languages of the World. Fifteenth Edition, SIL International, Dallas, TX (2005)
6. Tahir, T., Gence, C., et al.: Early software defects density prediction: training the international software benchmarking cross projects data using supervised learning. IEEE Access **11**, 141965–141986 (2023)
7. Cevik, T., et al.: Facial recognition in hexagonal domain – a frontier approach. IEEE Access **11**, 46577–46591 (2023)
8. Waziry, S., et al.: Performance comparison of machine learning driven approaches for classification of complex noises in quick response code images. Heliyon **9**(4) (2023)
9. Ahuja, R., et al.: Convolutional neural network based American sign language static hand gesture recognition. Int. J. Ambient Comput. Intell. **10**(3), 60–73 (2019)
10. Abdulhussein, A.A., Raheem, F.A.: Hand gesture recognition of static letters American sign language (ASL) using deep learning. Eng. Technol. J. **38**(6), 926–937 (2020)
11. Bhagat, N.K., Vishnusai, Y., Rathna, G.N.: Görüntü İşleme ve Derin Öğrenmeyi Kullanarak Hint İşaret Dili Hareket Tanıma. In: 2019 Digital Image Computing: Techniques and Applications (DICTA), pp. 1–8 (2019)
12. Sevli, O., Kemaloğlu, N.: Turkish sign language digits classification with CNN using different optimizers. Int. Adv. Res. Eng. J. **4**(3), 200–207 (2020)
13. Núñez Fernández, D., Kwolek, B.: Hand posture recognition using convolutional neural network. In: Mendoza, M., Velastín, S. (eds.) Progress in Pattern Recognition, Image Analysis, Computer Vision, and Applications (CIARP 2017). LNCS, vol. 10657, pp. 441–449. Springer, Cham (2018). https://doi.org/10.1007/978-3-319-75193-1_53
14. Rahmat, R.F., et al.: A study on dynamic hand gesture recognition for finger disability using multi-layer neural network. J. Theor. Appl. Inf. Technol. **96**(11), 3413–3425 (2018)
15. Wadhawan, A., Kumar, P.: Deep learning-based sign language recognition system for static signs. Neural Comput. Appl. **32**(12), 7957–7968 (2020)

16. Saleh, Y., Issa, G.F.: Arabic sign language recognition through deep neural networks fine-tuning.: Int. J. Online Biomed. Eng. **16**(5), 71–83 (2020)
17. Mathur, A., Singh, D., Chhikara, R.: Recognition of American sign language using deep learning. In: 2021 International Conference on Industrial Electronics Research and Applications (ICIERA), pp. 1–5. IEEE (2021)
18. Chung, H.Y., Chung, Y.L., Tsai, W.F.: An efficient hand gesture recognition system based on deep CNN. In: 2019 IEEE International Conference on Industrial Technology (ICIT). IEEE (2019)
19. Al-Hammadi, M., et al.: Hand gesture recognition for sign language using 3DCNN. IEEE Access **8**, 491–505 (2020)
20. Wangchuk, K., Riyamongkol, P., Waranusast, R.: Real-time Bhutanese sign language digits recognition system using convolutional neural network. ICT Express **7**(2), 215–220 (2021)
21. Islam, S., Mousumi, S.S.S., Rabby, A.S.A., Hossain, S.A., Abujar, S.: A potent model to recognize Bangla sign language digits using convolutional neural network. Procedia Comput. Sci. **143**, 611–618 (2018)
22. Barbhuiya, A.A., Karsh, R.K., Jain, R.: CNN based feature extraction and classification for sign language. Multimed. Tools Appl. **80**(2), 3051–3069 (2021)
23. Bengio, Y.: Learning deep architectures for AI. Found. trends® Mach. Learn. **2**(1), 1–127 (2021)
24. Liang, G., Hong, H., Xie, W., Zheng, L.: Combining convolutional neural network with recursive neural network for blood cell image classification. IEEE Access **6**, 36188–36197 (2018)
25. Zarándy, Á.: The art of CNN template design. Int. J. Circuit Theory Appl. **27**(1), 5–23 (1999)
26. Albawi, S., Mohammed, T.A., Al-Zawi, S.: Understanding of a convolutional neural network, 2017. In: 2017 International Conference on Engineering and Technology (ICET), vol. 10, pp. 1–6 (2017)
27. Andonie, R., Florea, A.C.: Weighted random search for CNN hyperparameter optimization (2020). arXiv preprint arXiv:2003.13300

Calculation of Bit-Error Probability for Direct-Sequence Spread-Spectrum Communications with Multiple-Access Interference of Rayleigh Distribution

Mohammed Albekairi(✉)

Department of Electrical Engineering, College of Engineering, Jouf University, Sakakah, Saudi Arabia
msalbekairi@ju.edu.sa

Abstract. Even with a small user base, recent cellular mobile systems showed capacity saturation in major urban areas. Further generations of wireless systems will offer higher data rates and flexibility. This demand required a large capacity increase. Multiple digital methods were used to solve the cellular mobile system capacity problem. Different users can share a fixed-spectrum resource using two digital strategies. One uses different frequencies (FDMA), and the other uses different time slots (TDMA). FDMA, TDMA, and hybrid capacities are well-defined. When RF channels or time slots are unavailable, no more customers can be served. Military applications of spread spectrum (SS) have been successful for decades. This spread spectrum uses Code Division Multiple Access, a new multiple access method. CDMA's higher capacity and multipath resistance make it an attractive scheme. The biggest factor limiting CDMA capacity is Multiple Access Interference (MAI). In this paper, we examine how MAI affects DS-CDMA system Bit Error Probability. Many methods have been reported for calculating the DS-CDMA bit error probability. They include three methods: Standard Gaussian Approximation (SGA), Improved Gaussian Approximation (IGA) and simplified IGA. These methods use the Central Limit Theorem (CLT), which approximates the MAI distribution as a Gaussian with a zero mean. We model MAI as a Rayleigh-distributed random variable. This model estimates the average BEP in an asynchronous DS-CDMA system well. SGA with a nonzero mean is used to compare our methods to previous work.

Keywords: Bit Error Probabilities · Code-Division Multiple-Access · Multiple Access Interference · Rayleigh Distribution

1 Introduction

Today, mobile communications are in high demand. Due to their use of traditional multiple access techniques (FDMA, TDMA, or a combination of them), existing mobile systems like AMPS and GSM have limited capacity. Urban business areas' severe mobile communication spectrum congestion highlights the need for a new cellular system that

J. Rasheed et al. (Eds.): FoNeS-AIoT 2024, LNNS 1035, pp. 11–21, 2024.
https://doi.org/10.1007/978-3-031-62871-9_2

uses the spectrum more efficiently. Spread spectrum (SS) communications began in the 1950s for military guidance and communication. The SS technique is named so because its transmitted bandwidth is much larger than the minimum needed to send information. SS was initially used for its noise and jamming resistance. As a multiple-access technique, the spread spectrum technique is very convenient. CDMA is a multiple-access method [1–5]. CDMA was created as a hybrid of time slots and frequency bands. The goal is to address mobile telecommunications capacity shortages. CDMA allows multiple users to share the same frequency band without interfering if mobile station (MS) transmitted power is carefully controlled. All neighboring cells can use the same frequency. BSs can serve an unlimited number of active users. When active users exceed the design value, service quality can be lowered to provide more traffic channels. Usually called soft capacity. Thus, CDMA systems may have unlimited capacity [6].

Digital communications systems like cell phones and wireless personal communications use CDMA technology. Commercial CDMA technology improves capacity, coverage, and voice quality, creating a new generation of wireless networks.

Multiple users can transmit over the same radio frequency (RF) bandwidth with SS multiple access techniques like CDMA. Different users' spread signals interfere unless their transmissions are perfectly synchronized and orthogonal spreading sequences (codes) are used. In most practical wireless systems, user synchronization is difficult in uplinks, and we may not want to use orthogonal codes. Thus, some users' interference with others may cause multiple access interference (MAI) [7]. We want to study how MAI affects communication system performance. MAI is the main factor limiting system performance and capacity. Thus, CDMA research has focused on MAI's impact on system performance. Bit error probability (BEP) measures this effect on system performance [8–12].

It is hard to figure out how well DS-CDMA systems with the matched filter receiver work for bit error even when there is additive white Gaussian noise (AWGN) in the channel. Usually, we use limits and approximations. The standard Gaussian approximation (SGA) is one of the most popular [13]. This approximation uses a central limit theorem (CLT) to approximate the sum of the MAI signals as an additive white-Gaussian process with zero mean additional to the background Gaussian noise process. This receiver uses a conventional single-user-matched filter (correlation receiver) to detect the desired user signal. The filter's output signal-to-noise ratio (SNR) is calculated using the MAI's average variance overall operating conditions.

Due to its simplicity, the SGA is widely used, but performance analyses based on it often overestimate system performance, especially when the number of users is small. Some derivatives of the SGA have been proposed to overcome these limitations, in particular the Improved Gaussian approximation (IGA) and the Simplified IGA (SIGA).

This paper looks at how MAI affects BEP performance in DS-CDMA systems with users that are spread out and interfere, and it comes up with a good estimate. A reanalysis of the SGA with a non-zero mean is also examined. Consider all relevant calculation methods and compare our results (MAI with Rayleigh distribution) to all others. We consider this distribution for MAI because the Rayleigh distribution is often used in mobile radio channels to describe the statistical time-varying received envelope of a flat fading signal or a multipath component. It is well known that the envelope of the sum of two quadrature Gaussian interfering signals follows a Rayleigh distribution. Additionally, this distribution describes radar target detection techniques' fluctuation. In this paper, the MAI is assumed to be the only source of bit errors, but additive white Gaussian noise (AWGN) can be included.

This paper is organized as follows: Sect. 2 introduces the mathematical foundations allowing the MAI to be considered as a Rayleigh distributed random variable. Section 3 shows experimental results and performance interpretation. Finally, Sect. 4 outlines the main contribution of this work and the future challenges.

2 MAI as a Rayleigh Distributed Random Variable

In mobile radio channels, the Rayleigh distribution is commonly used to describe the statistically time-varying nature of the received envelope of a flat-fading signal or the envelope of an individual component of a multipath. It is well known that the envelope of the sum of two quadrature Gaussian interfering signals obeys a Rayleigh distribution [14]. Moreover, this distribution describes the fluctuating nature of radar target detection techniques. Our object in this section is to calculate the BEP based on the assumption that the MAI is modeled as a random variable with a Rayleigh distribution that has a probability density function (pdf) of the form [15]:

$$f_{\psi_n}(\psi_n) = \frac{\psi_n}{\alpha^2}\, e^{-\psi_n^2/2\alpha^2} \qquad \psi_n \geq \ 0 \tag{1}$$

where ψ_n represents the interference introduced by the nth user. The intensity of that interference may vary from one user to another. To simplify our mathematical analysis, the characteristic function (CF) of this distribution must first be calculated because it plays an important part in handling our computation of BEP. The characteristic function (CF) corresponding to this pdf is defined as:

$$F_{\psi_n}(\omega) \ = \int_{-\infty}^{\infty} f_{\psi_n}(\psi_n)\, e^{-j\omega\psi_n} d\,\psi_n \tag{2}$$

$$F_{\psi_n}(\omega) \ = \int_{0}^{\infty} \frac{\psi_n}{\alpha^2}\, e^{-\psi_n^2/2\alpha^2}\, e^{-j\omega\psi_n} d\,\psi_n \tag{3}$$

$$F_{\psi_n}(\omega) = \int_{0}^{\infty} \frac{\psi_n}{\alpha^2} e^{-\psi_n^2/2\alpha^2} \cos\ \psi_n\omega\ \ d\,\psi_n - j\int_{0}^{\infty} \frac{\psi_n}{\alpha^2} e^{-\psi_n^2/2\alpha^2} \sin\ \ \psi_n\omega\ \ d\,\psi_n \tag{4}$$

The integration of the second term is given by:

$$\int_{0}^{\infty} \frac{\psi_n}{\alpha^2} e^{-\psi_n^2/2\alpha^2} \sin\ \ \psi_n\omega\ \ d\,\psi_n = \sqrt{\frac{\pi}{2}}\,\alpha\omega e^{-\omega^2\alpha^2/2} \tag{5}$$

while the first integration term is:

$$\int_0^\infty \frac{\psi_n}{\alpha^2} e^{-\psi_n^2/2\alpha^2} \cos\ \psi_n\omega\ \ d\psi_n\ = 1 - (\omega\alpha)^2 + \frac{(\omega\alpha)^4}{3} - \frac{(\omega\alpha)^6}{3\,.5} + \frac{(\omega\alpha)^8}{3\,.5\,.7} + \ldots \quad (6)$$
$$\approx e^{-(\omega\alpha)^2}$$

Then, Eq. (4) can be expressed as:

$$F_{\psi_n}(\omega) \approx e^{-(\omega\alpha)^2} - j\sqrt{\frac{\pi}{2}}\alpha\omega\ e^{-\omega^2\alpha^2/2} \quad (7)$$

The BEP can be calculated directly from:

$$P_e = \frac{1}{2}\int_{I_0}^{\infty} p_\psi(\psi)d\psi \quad (8)$$

where $p_\psi(\psi)$ is the joint pdf of the (k − 1) users. The ω-domain representation is given by:

$$P_\psi(\omega)\ =\ F_{\psi_1}(\omega)F_{\psi_2}(\omega)\cdots F_{\psi_{k-1}}(\omega) \quad (9)$$

If the interference produced by (k − 1) users is i.i.d. (Independent and Identically Distributed), the above equation can be simplified to

$$P_\psi(\omega)\ =\ \left[F_\psi(\omega)\right]^{k-1} \quad (10)$$

Substituting Eq. (7) into Eq. (10), gives

$$P_\psi(\omega)\ =\ \left[e^{-(\omega\alpha)^2} - j\sqrt{\frac{\pi}{2}}\alpha\omega\ e^{-\omega^2\alpha^2/2}\right]^{k-1}$$
$$= \sum_{\ell=0}^{k-1}\binom{k-1}{\ell}\left(\sqrt{\frac{\pi}{2}}\alpha\right)^{\ell}(-1)^{\ell}(j\omega)^{\ell}\left(e^{-\omega^2\alpha^2}\right)^{k-1-\frac{\ell}{2}} \quad (11)$$

Based on the properties of the Fourier transform [16]:

$$(j\omega)^{\ell}M(\omega) \Leftrightarrow \frac{d^{\ell}}{d\psi^{\ell}}(m(\psi)) \quad (12)$$

Let $M(\omega) = \left(e^{-\omega^2\alpha^2}\right)^{k-1-\frac{\ell}{2}}$ then:

$$m(\psi) = \frac{1}{\alpha\sqrt{4\pi\left(k-1-\frac{\ell}{2}\right)}} e^{-\psi^2/4\alpha^2\left(k-1-\frac{\ell}{2}\right)} \quad (13)$$

Substituting Eq. (13) into Eq. (12), the inverse Fourier transform of Eq. (11) can be evaluated as, ℓ th derivation of $m(\psi)$ w.r.t. ψ. In other words:

$$\frac{d^\ell}{d\psi^\ell}(m(\psi)) = \frac{d^\ell}{d\psi^\ell}\left(\frac{1}{\alpha\sqrt{4\pi\left(k-1-\frac{\ell}{2}\right)}}e^{-\psi^2/4\alpha^2\left(k-1-\frac{\ell}{2}\right)}\right) \tag{14}$$

The key to simplification of the resulting formula is the Hermite polynomial, which is defined as:

$$H_\ell(x) = (-1)^\ell e^{x^2}\frac{d^\ell}{dx^\ell}\left(e^{-x^2}\right) \tag{15}$$

$H_\ell(x)$ is called a Hermite polynomial. Rearranging the equation to become:

$$\frac{d^\ell}{dx^\ell}\left(e^{-x^2}\right) = (-1)^{-\ell}e^{-x^2}H_\ell(x) \tag{16}$$

Now, let $x = \frac{\psi}{2\alpha\sqrt{k-\frac{\ell}{2}}}$.

The using of the developed polynomial in Eq. (14) makes it as

$$\frac{d^\ell}{d\psi^\ell}\left(e^{-\psi^2/4\alpha^2\left(k-1-\frac{\ell}{2}\right)}\right) = (-1)^{-\ell}\left(\frac{1}{2\alpha\sqrt{k-1-\frac{\ell}{2}}}\right)^\ell e^{-\psi^2/4\alpha^2\left(k-1-\frac{\ell}{2}\right)}H_\ell\left(\frac{\psi}{2\alpha\sqrt{k-1-\frac{\ell}{2}}}\right) \tag{17}$$

Using, the pdf of ψ can be easily evaluated as:

$$p_\psi(\psi) = \sum_{\ell=0}^{k-1}\binom{k-1}{\ell}\left(\sqrt{\frac{\pi}{2}}\alpha\right)^\ell(-1)^\ell\frac{1}{\alpha\sqrt{4\pi\left(k-1-\frac{\ell}{2}\right)}}(-1)^{-\ell}\left(\frac{1}{2\alpha\sqrt{k-1-\frac{\ell}{2}}}\right)^\ell e^{-\psi^2/4\alpha^2\left(k-1-\frac{\ell}{2}\right)}H_\ell\left(\frac{\psi}{2\alpha\sqrt{k-1-\frac{\ell}{2}}}\right) \tag{18}$$

Substituting Eq. (18) into Eq. (8), the average BEP is found to be

$$P_e = \sum_{\ell=0}^{k-1}\binom{k-1}{\ell}\frac{1}{\alpha\sqrt{16\pi\left(k-1-\frac{\ell}{2}\right)}}\left(\sqrt{\frac{\pi}{2}}\alpha\right)^\ell\left(\frac{1}{2\alpha\sqrt{k-1-\frac{\ell}{2}}}\right)^\ell\int_{I_0}^{\infty}e^{-\psi^2/4\alpha^2\left(k-1-\frac{\ell}{2}\right)}H_\ell\left(\frac{\psi}{2\alpha\sqrt{k-1-\frac{\ell}{2}}}\right)d\psi \tag{19}$$

Since the above integral equation has no closed form, we calculate it numerically.

3 Experimental Results

In this section, we are interested in assessing the obtained analytical results to show the validity of our proposed model. The numerical results given here are evaluated for the most important parameter α^2. This value is calculated as $\alpha^2 = \frac{\sigma_\varsigma^2}{2-\frac{\pi}{2}}$, where:

$$\sigma_\varsigma^2 = \frac{NT_c^2}{6}\sum_{n=1}^{k-1}P_n \tag{20}$$

$T_c = 1$ and $P_0 = P_1 = \ldots = P_{k\text{-}1} = 2$.

Figure 1 shows the variation of BEP with the number of users K. The curves in this figure are parametric in N (processing gain). As the processing gain increases, the BEP decreases. This behavior is logical since increasing the processing gain increases the immunity of the system to interference, and correspondingly, the BEP becomes lower than in the case of smaller processing gains. The results of Fig. 1 demonstrate this statement.

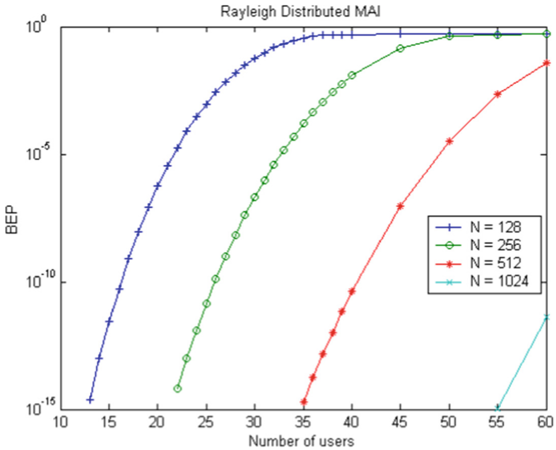

Fig. 1. Bit error probability as a function of the total number of users for N = 128, 256, 512, and 1024 when MAI obeys the Rayleigh distribution $\alpha^2 = \sigma_\varsigma^2 \big/ 10\left(2 - \frac{\pi}{2}\right)$.

It is important to note that the family of curves of this figure is drawn for: $\alpha^2 = \frac{\sigma_\varsigma^2}{2-\frac{\pi}{2}}$, $\alpha^2 = \frac{\sigma_\varsigma^2}{10\left(2-\frac{\pi}{2}\right)}$, and $\alpha^2 = \frac{\sigma_\varsigma^2}{20\left(2-\frac{\pi}{2}\right)}$.

To show this effect of α^2 on the behavior of BEP, we redraw the curves of Fig. 1 for smaller and greater values of α^2, as indicated in Fig. 2 and Fig. 3 respectively. As the results of these figures demonstrate, the parameter α^2 plays an important role in determining the BEP as a function of the number of users. When α^2 has smaller values, the BEP has correspondingly smaller values. This is predicated since smaller α^2 means smaller variance of MAI. In other words, increasing α^2 will give higher values for BEP. In any case, BEP increases as the number of users increases because increasing the number of users means increasing the effect of MAI on the desired user. The variance of MAI affects the values of BEP directly. To demonstrate this statement, we plot BEP as a function of K for different values of this variance, and the results are shown in Fig. 4. The family of curves in this figure has the same behavior, with the exception that as the variance increases, the start of its corresponding curves is shifted towards a larger number of users. The asymptotic value of BEP is approximately 50% in any case. To reduce the effect of this variance, one of the proposed solutions is to increase the processing gain. This conclusion is depicted in Fig. 5.

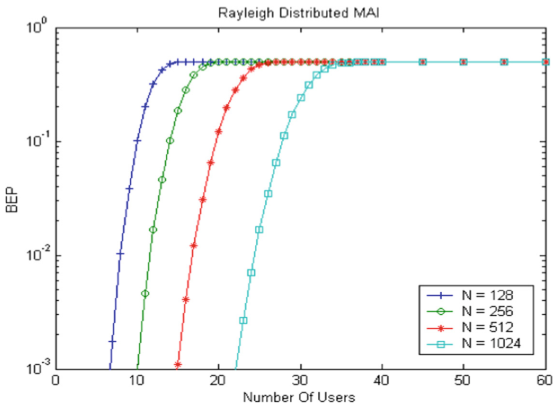

Fig. 2. Bit error probability as a function of the total number of users for N = 128, 256, 512, and 1024 when MAI obeys the Rayleigh distribution with $\alpha^2 = \sigma_\varsigma^2 \Big/ \left(2 - \frac{\pi}{2}\right)$.

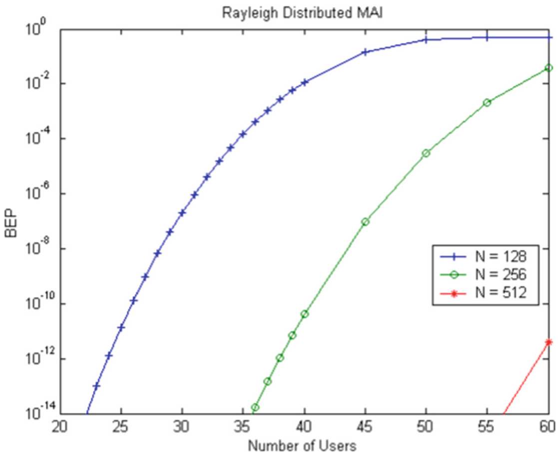

Fig. 3. Bit error probability as a function of the total number of users for N = 128, 256, 512, and 1024 when MAI obeys the Rayleigh distribution with $\alpha^2 = \sigma_\varsigma^2 \Big/ 20\left(2 - \frac{\pi}{2}\right)$.

To compare our proposed model with the previously evaluated techniques, we calculate some values of BEP using our technique and preview techniques. The results are displayed in Fig. 6(a) for N = 128 and $\alpha^2 = \sigma_\varsigma^2 \Big/ \left(2 - \frac{\pi}{2}\right)10$.

Based on this figure, we can show that the Rayleigh fading channel gives the highest BEP values when the number of users is small. As the number of users increases, the BEP also increases, with a rate that varies depending on the processing technique. The reference (practical) technique has the highest rate until the number of users reaches 17, beyond which our technique gives higher values than SGA with a non-zero mean. These higher values remain until the number of users reaches 28, beyond which the two techniques give the same value for BEP, which is higher than that obtained with

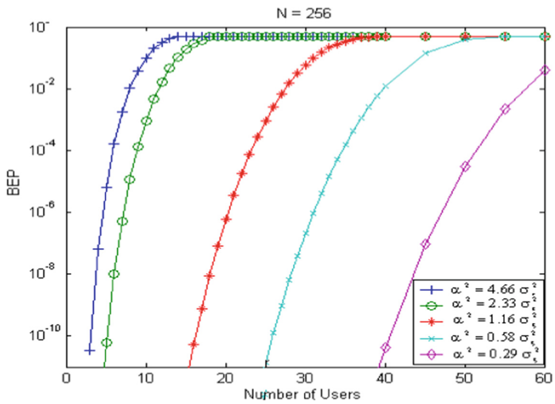

Fig. 4. Variation of BEP with K as a function of α^2 when N = 256.

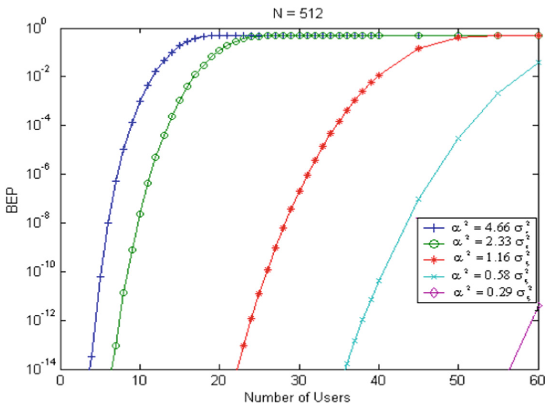

Fig. 5. Variation of BEP with K as a function of α^2 when N = 512.

the reference and the Rayleigh fading channel techniques. On the other hand, the SGA with a zero mean has smaller values for BEP. Since the proposed Rayleigh distribution has a nonzero mean, it is evident that the nearest approach to it is the SGA with a nonzero mean. For smaller values of K, the distribution gives smaller values for BEP than those obtained by SGA with a nonzero mean. As the number of users increases, the two approaches give the same values of BEP. This behavior is logical according to the central limit theorem, which states that the sum of a specified number of independent RVs in any distribution tends to be a Gaussian distribution. The curves in this figure are drawn for fixed values of processing gain and the variance of MAI. To show the effect of the variance of MAI on the behavior of these curves, we repeat them for another value of α^2 as shown in Fig. 6(b). In this case, we note that the reference (practical) technique has the highest rate until the number of users reaches 28, beyond which our technique gives higher values than SGA with a non-zero mean. These higher values remain until the number of users reaches 40, beyond which the two techniques give the same value for BEP, which is higher than that obtained with the reference and the Rayleigh fading channel techniques. To show the effect of the processing gain on the behavior of these curves, we repeat them for another value of N, as shown in Fig. 6(c) and Fig. 6(d). Based on the analysis of these figures, it can be inferred that the SGA with an average value of zero is not feasible. This is attributed to the fact that the mean of the Multiple Access Interference (MAI) does not equal zero, rendering the Signal-to-Interference-plus-Noise Ratio (SINR) with a zero mean as invalid.

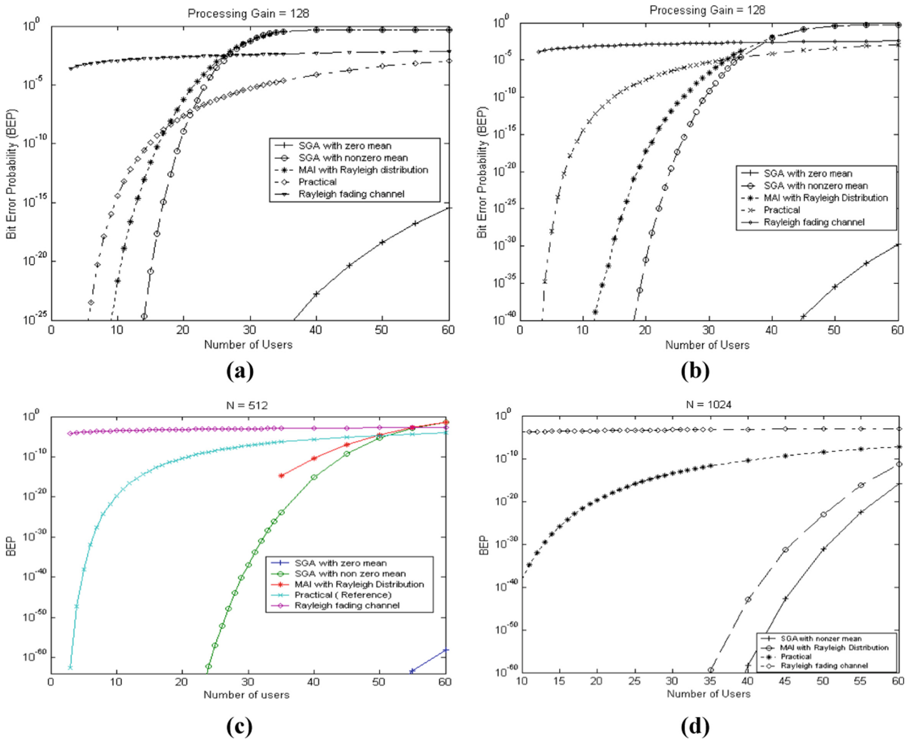

Fig. 6. Comparison of BEP results, evaluated for different processing techniques when: **(a)**$\alpha^2 = \sigma_\varsigma^2 \Big/ \left(2 - \frac{\pi}{2}\right)10$ and N = 128, **(b)** $\alpha^2 = \sigma_\varsigma^2 \Big/ \left(2 - \frac{\pi}{2}\right)20$ and N = 128, **(c)** $\alpha^2 = \sigma_\varsigma^2 \Big/ \left(2 - \frac{\pi}{2}\right)10$ and N = 512, **(d)** $\alpha^2 = \sigma_\varsigma^2 \Big/ \left(2 - \frac{\pi}{2}\right)10$ and N = 1024.

4 Conclusion

The Rayleigh distribution, a new MAI distribution, is proposed in this paper. For this distribution, we analyze errors caused by other users for the desired user. Calculating the CF of the proposed distribution, the basis of our analysis, yields a nearly exact BEP formula. Our numerical results prove the proposed distribution is valid for small user numbers. According to the CLT, the large number of interfering users tends to have a

Gaussian distribution. BEP behavior depends on some parameters. MAI variance and processing gain are examples. We examined how processing gain and MAI variance affect BEP. When processing gain rises, BEP falls. This is logical because increasing processing gain increases system immunity to interference and lowers BEP. Increasing MAI variance raises BEP. For smaller user numbers, our model's numerical values are closest to the standard curve. Instead of single-user detection, we can expand our research to include multi-user detection.

References

1. Lin, M.-C., Lee, S.-K., Fan, H.-H., Chen, Y.-H.: GDMA, LDS-CDMA, and HDS-CDMA for uplink communication systems. In: 2023 VTS Asia Pacific Wireless Communications Symposium (APWCS) (2023). https://doi.org/10.1109/apwcs60142.2023.10234063
2. Ma, T., Xiao, Y., Lei, X., Xiong, W., Xiao, M.: Spreading CDMA via RIS: multipath separation, estimation, and combination. IEEE Internet Things J. **10**(13), 11396–11413 (2023). https://doi.org/10.1109/jiot.2023.3242864
3. Shen, Y., Xu, Y.: Multiple-access interference and multipath influence mitigation for multicarrier code-division multiple-access signals. IEEE Access **8**, 3408–3415 (2020). https://doi.org/10.1109/access.2019.2962633
4. Moinuddin, M., Zerguine, A., Sheikh, A.: Multiple-access interference plus noise-constrained least mean square (MNCLMS) algorithm for CDMA systems. IEEE Trans. Circuits Syst. I Regul. Pap. **55**(9), 2870–2883 (2008). https://doi.org/10.1109/tcsi.2008.923166
5. Torrieri, D.: Principles of Spread-Spectrum Communication Systems. Springer, Cham (2022). https://doi.org/10.1007/978-3-319-14096-4
6. Evans, J., Everitt, D.: Infinite server traffic models for CDMA cellular mobile networks. In: Jabbari, B., Godlewski, P., Lagrange, X. (eds.) Multiaccess, Mobility and Teletraffic for Personal Communications. The Kluwer International Series in Engineering and Computer Science, vol. 366. Springer, Boston (1996). https://doi.org/10.1007/978-1-4613-1409-7_12
7. Mahmood, K., Asad, S.M., Moinuddin, M., Zerguine, A., Cheded, L.: Multiple access interference in MIMO-CDMA systems under Rayleigh fading: statistical characterization and applications. EURASIP J. Adv. Sig. Process. **2016**(1), (2016). https://doi.org/10.1186/s13634-016-0338-y
8. Kaddoum, G., Chargé, P., Roviras, D., Fournier-Prunaret, D.: A methodology for bit error rate prediction in chaos-based communication systems. Circuits Syst. Signal Process. **28**(6), 925–944 (2009). https://doi.org/10.1007/s00034-009-9124-5
9. Zhang, L., Lu, H., Wu, Z., Jiang, M.: Bit error rate analysis of chaotic cognitive radio system over slow fading channels. Ann. Telecommun. Annales des Télécommunications **70**(11–12), 513–521 (2015). https://doi.org/10.1007/s12243-015-0472-9
10. Fujisaki, H., Yamada, Y.: On bit error probabilities of SSMA communication systems using spreading sequences of Markov chains. In: Eighth IEEE International Symposium on Spread Spectrum Techniques and Applications - Program and Book of Abstracts (IEEE Cat No. 04TH8738) (2004). https://doi.org/10.1109/isssta.2004.1371842
11. Fujisaki, H., Keller, G.: Approximations for bit error probabilities in SSMA communication systems using spreading sequences of Markov chains. In: 2005 IEEE International Symposium on Circuits and Systems (2005)
12. Ding, X., Xiong, H., Gong, S., Peng, M., Tang, J.: M-ary orthogonal signal and BER performance in wireless communication systems. In: 2018 IEEE 4th International Conference on Computer and Communications (ICCC) (2018). https://doi.org/10.1109/compcomm.2018.8780668

13. Luque, J.R., Morón, M.J., Casilari, E.: Analytical and empirical evaluation of the impact of Gaussian noise on the modulations employed by bluetooth enhanced data rates. EURASIP J. Wirel. Commun. Netw. **2012**(1), (2012). https://doi.org/10.1186/1687-1499-2012-94
14. Rappaport, T.S.: Wireless Communications: Principles and Practice. Prentice Hall Communications Engineering and Emerging Technologies Series, 2nd edn. Prentice Hall, Hoboken (2002)
15. Vorobiyenko, P., Ilchenko, M., Strelkovska, I.: Current Trends in Communication and Information Technologies. Springer, Cham (2021). https://doi.org/10.1007/978-3-030-76343-5
16. Glover, I., Grant, P.M.: Digital Communications. Pearson Education, London (2010)